FOCUS: HONORING HELMUT SCHWARZ'S ELECTION TO THE NATIONAL ACADEMY OF SCIENCES: RESEARCH ARTICLE

Ligation Kinetics as a Probe for Non-Covalent Electrostatic Bonding and Electron Solvation of Alkali and Alkaline Earth Cations with Ammonia

Voislav Blagojevic, Vitali V. Lavrov, Gregory K. Koyanagi, Diethard K. Bohme [ORCID]

Department of Chemistry, Centre for Research in Mass Spectrometry and Centre for Research in Earth and Space Science, York University, Toronto, Ontario M3J 1P3, Canada
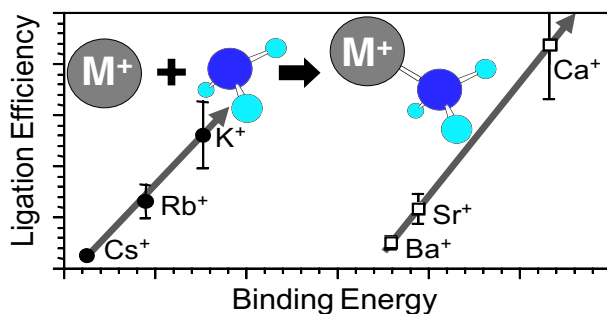
Abstract. Mono-ligation kinetics were measured for ammonia reacting with atomic cations in the first two groups of the periodic table (K^+, Rb^+, Cs^+ and Ca^+, Sr^+, Ba^+). Also, mono-ligation energies were computed using density functional theory (DFT) in an attempt to assess the role of non-covalent electrostatic interactions in these chemical reactions. The measurements were performed at room temperature in helium bath gas at 0.35 Torr using an inductively coupled plasma/ selected-ion flow tube (ICP/SIFT) tandem mass spectrometer. Rate coefficients are reported for ammonia addition, the only reaction channel that was observed with all these cations. A systematic decrease in the rate of addition of NH_3 was observed for both group 1 and 2 cations going down the periodic table. The computational studies predict a decrease in the adduct binding energy and an increase in the bond separation going down groups 1 and 2 of the periodic table and provide some insight into the role of the extra selectron in the group 2 radical cations in ligand bonding. A correlation is seen between the efficiency of ligation and the binding energy of the adduct ion and attributed to the lifetime of the intermediate encounter complex against back dissociation which is dependent on its well depth. Higher-order additions of ammonia were also observed. Remarkable differences in the extent and kinetics were seen between the group 1 and 2 cations, and these were attributed to the occurrence of ammonia solvation of the extra s electron in the higher-order adducts of the alkaline earth cations.

Keywords: Ligation of K^+, Rb^+, Cs^+, Ca^+, Sr^+ and Ba^+, Periodic trends in ion kinetics, Ammonia, Electron solvation, ICP/SIFT technique

Introduction

Our recent measurements of magnitudes and trends in the ligation kinetics of atomic cations [1–5] have

---

Dedicated to Helmut Schwarz on his election to the National Academy of Science

---

Electronic supplementary material The online version of this article (https://doi.org/10.1007/s13361-019-02234-2) contains supplementary material, which is available to authorized users.

Correspondence to: Diethard Bohme; *e-mail:* dkbohme@yorku.ca

demonstrated that these can provide a valuable probe of the nature of the bonding between atomic cations and small ligand molecules across and down the periodic table. Both relativistic effects [1–3] and ligand-field stabilization [4] were shown to contribute to the bonding of ligands to atomic transition metal cations. For example, earlier studies of ammonia ligation with group 10 [1] and 11 [2] atomic transition metal cations showed a strong rate enhancement with the third-row cations Pt^+ and Au^+ that could be attributed to relativistic effects in ammonia bonding. Also, we observed trends more recently in the rate coefficients for the ligation of group 12 atomic transition metal cations with other small molecular ligands; a strong rate

enhancement was observed going down the period for the ligation of Hg^+ that also could be attributed to relativistic effects that enhance the stability of these ligated cations [3]. Our recent measurements of the kinetics of ammonia ligation to first- and second-row atomic transition metal cations were able to assess the role of ligand-field stabilization energy, LFSE [4]. Early atomic transition metal cations were seen in a separate study to induce N–H bond insertions once, and even twice, in bond redisposition reactions leading to imide ions by H_2 elimination and to do so more extensively going down the periodic table [5]. Our measurements of ammonia reactions with 14 atomic lanthanide cations for which $La^+(5d^2)$, $Ce^+(4f^1 5d^2)$, $Gd^+(4f^7 5d^1 6s^1)$, and $Tb^+(4f^9 6s^1)$ exhibited bond redisposition to form the protonated lanthanide nitride $LnNH^+$ [6]. Apparently, the electrostatic attraction between the atomic lanthanide cation and ammonia is sufficiently strong only in these latter reactions to provide enough energy to achieve a $5d^1 6s^1$ configuration by electron promotion that permits exothermic N–H bond insertion with H_2 elimination.

Here, we focus on non-covalent interactions. We explore the influence of the strength of electrostatic bonding on the kinetics of exclusive ligation reactions down the periodic table. Of course, the group 1 and 2 cations provide the obvious atomic cations of choice for such a study. Group 1 cations have a rare-gas atom configuration, and the group 2 radical cations provide an additional s^1 electron shielding a doubly charged core available for electrostatic bonding. Our inductively coupled plasma (ICP) source in our ICP/selected-ion flow tube (SIFT) apparatus allows access to most of these cations in both of these groups. Also, we have previously measured the rate of ligation of Mg^+ with ammonia using more conventional electron-impact ionization of magnesocene to produce Mg^+ [7].

It seems that ammonia is uniquely suited as a reagent ligand: its substantial dipole moment (1.470 D) [8] and polarizability (2.16 $Å^3$) [8] favor electrostatic bonding; its ionization energy, $IE(NH_3) = 10.07$ eV [9], avoids electron transfer, and it is chemically quite robust in that the N–H bond is relatively strong. Our previous measurements with small non-polar molecules (that do not undergo bimolecular reactions), methane [10], and carbon dioxide [11] showed that both group 1 and 2 cations exhibited rates of ligation too small to measure with our instrumentation.

In the gas phase (in a helium bath, for example), the gas-phase formation of ligated atomic cations M^+L (where L is the ligand) occurs via two steps: formation of an encounter complex and its subsequent collisional stabilization by the bath gas.

$$M^+ + L \underset{K_{-1}}{\overset{K_1}{\rightleftarrows}} (M^+-L)^*$$

$$(M^+-L)^* + He \overset{k_s}{\rightarrow} M^+-L + He$$
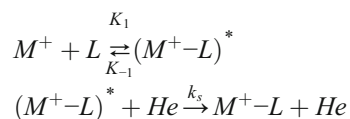
The third-order rate coefficient for the overall ligation $k(3) = k_1 k_s/k_{-1}$ can be derived when applying the steady-state assumption to the encounter complex $(M^+-NH_3)^*$. For the unimolecular dissociation of the encounter complex back to

reactants, k_{-1} is a frequency or the inverse of the lifetime, τ_1^{-1}. Classical statistical theories predict that the lifetime for unimolecular decomposition τ is related to the binding energy (well depth) D of the encounter complex according to $\tau = \tau_0 ((D + rRT)/rRT)^{s-1}$ [12]. Here, τ_0 is the collision lifetime (the inverse of the vibrational frequency along the reaction coordinate), r is the number of energy squared terms contributing to the internal energy of the molecule, and s is the number of coupled harmonic oscillators in the encounter complex. So, the rate coefficient for ligation k is related to the binding energy. When comparisons are made down a group of atomic metal cations attaching to the *same* ligand, primarily the binding energy, and not the degrees of freedom or the number of energy square terms, will be decisive and trend setting. Both k_1 and $k_s(k_c)$ decrease with increasing mass of the cation, and only slightly, 15% going from K^+ to Cs^+ or Ca^+ to Ba^+ ($k_s = P \times k_c$ where k_c is the collision rate coefficient, and P is the probability of stabilization which we assume to be constant for each group).

In the study reported here, we have probed the ligation of the group 1 (Rg) cations K^+, Rb^+, and Cs^+ and the group 2 (Rg s^1) cations Ca^+, Sr^+, and Ba^+ with rate coefficient measurements using ammonia as the ligand. Computations with density functional theory (DFT) using relativistic effective core potentials (ECPs) were performed to predict the binding energies with this ligand, and these are correlated with our measured ligation efficiencies. The rare-gas configurations of the group 1 cations lead to non-covalent, purely electrostatic interactions whereas the extra s electron in the group 2 radical cations presents an intriguing perturbation to the pure electrostatic interaction.

Experimental

The experimental results reported here were obtained with the ICP/SIFT tandem mass spectrometer that has been described in detail previously [13–15]. The atomic ions were generated within an atmospheric pressure argon plasma at 5500 K fed with a vaporized solution containing the metal salt. Solutions containing the metal salt of interest with concentration of ca. 5 μg L^{-1} were peristaltically pumped via a nebulizer into the plasma. The nebulizer flow was adjusted to maximize the ion signal detected downstream of the flow tube. The sample solutions were prepared using atomic spectroscopy standard solutions commercially available from SPEX, Teknolab, J.T. Baker Chemical Co., Fisher Scientific Company, Perkin-Elmer, and Alfa Products. Aliquots of standard solutions were diluted with highly purified water produced in the Millipore Milli-Q Plus ultra-pure water system. The final concentrations were varied between 5 and 20 ppm to achieve suitable intensity of the resultant ion beam. A stabilizing agent was usually added to each solution in order to prevent precipitation: KOH for base-stabilized salts and HNO_3 or HCl for acid-stabilized salts.

Atomic ions emerge from the ICP at a nominal plasma ion temperature of 5500 K with the corresponding Boltzmann distributions. After extraction from the ICP, the plasma ions may experience electronic-state relaxations via both radiative

decay and collisional energy transfer. The latter may occur by collisions with argon, as the extracted plasma cools upon sampling, and with helium in the flow tube (ca. 4×10^5 collisions with helium) prior to the reaction region. However, the exact extent of electronic relaxation is uncertain. Clues to the presence of excited electronic states of the atomic ions in the reaction region can be found in the product ions observed and in the shape of the semi-logarithmic decay of the reacting atomic ion upon addition of neutral reactants. Curvature will appear in the measured atomic-ion decay when the ground state and excited state react at different rates even when they give the same product ions. An excited-state effect cannot be seen when the products and reaction rates are the same for both the ground and excited states, but in this case, the measured atomic-ion decay defines the ground-state kinetics. There were no indications of excited state effects in the measurements reported here. The many collisions experienced by the atomic cations with the quite polarizable argon atoms as they emerge from the ICP and the ca. 4×10^5 collisions with helium atoms in the flow tube (the helium buffer gas pressure was 0.35 ± 0.01 Torr) appear to be sufficient to thermalize the excited states and to ensure that the atomic ions reach a translational temperature equal to the tube temperature of 295 ± 2 K prior to entering the reaction region.

Reactions of K^+, Rb^+, Cs^+, Ca^+, Sr^+, and Ba^+ were investigated with NH_3 at a helium buffer gas pressure of 0.35 ± 0.01 Torr and temperature of 295 ± 2 K. Reaction rate coefficients were determined in the usual manner using pseudo first-order kinetics [15].

Highly pure NH_3 gas was obtained commercially (semiconductor grade 99.999%, Matheson/Linde Canada) and introduced into the reaction region of the SIFT as a dilute (15%) mixture in helium.

Theory

Adducts of metal cations with ammonia were examined with DFT using relativistic ECPs. We used the Gaussian 03 suite of programs [16] with the B3LYP DFT method [17, 18] and the SDD basis set [19] on the metals centers and the D95 basis set on hydrogen and nitrogen [20]. Stationary points for the ammonia complexes were studied starting from fully flexible C1 symmetry initial geometries. Upon geometry optimization, the ammonia clusters fell into C_{3v} symmetry structures.

Results and Discussion

Experimental Results

The quality of our experimental measurements can be assessed from our experimental results in Figures 1 and 2 for ammonia ligation of K^+, Rb^+, Cs^+, Ca^+, Sr^+, and Ba^+ at room temperature in helium buffer gas at 0.35 ± 0.01 Torr. Ammonia addition was the only reaction channel that was observed in each case. Reactions with Li^+, Na^+, Be^+, and Mg^+ were not investigated
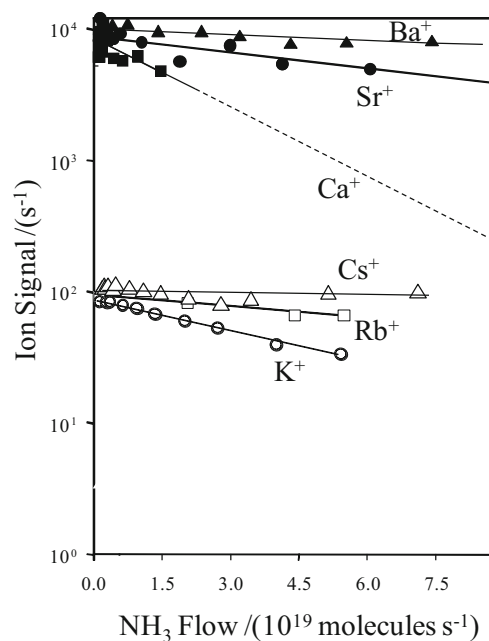
Figure 1. Ion decays monitored for the ligation of the bare alkali and alkali earth metal cations with ammonia in He buffer gas at 0.35 ± 0.01 Torr. Symbols represent experimental data and lines represent kinetic fits to that data

since the ICP source uses an argon plasma which is not an efficient source of light atomic ions [13, 14].

The change in the slopes of the six measured atomic cation decays shown in Figure 1 is an indication of the change in the rate coefficients for the primary ammonia addition. Clearly, the rate coefficient decreases systematically going down the periodic table for both the alkali and alkali earth atomic cations. The numerical values for the rate coefficients are summarized in Table 1. As shown in Figure 2, further higher-order additions of ammonia were observed for all six cations (see Table 1); up to as many as six ammonia molecules were observed to add to Ca^+, in the ammonia flow range and at the helium pressure investigated.

The ammonia ligation efficiencies in Table 1 are expressed as k/k_c where k_c is the collision rate coefficient calculated using available theory [21] with $\mu_D(NH_3) = 1.470$ D [8] and $\alpha(NH_3) = 2.16$ Å^3 [8].

Computational Results

Table 2 provides a summary of the computations performed for the ammonia ligation of group 1 and group 2 cations in the periodic table. The geometries of all adducts were computed to have C_{3v} symmetry. The metal-nitrogen equilibrium bond distances are seen to increase down the periodic table by about 14% for both group 1 and group 2 adduct ions with group 2 distances being shorter than the group 1 distances by about 13%.

Binding enthalpies are generally quite low, ΔH_{298} < 90.4 kJ mol^{-1} for group 1 adducts and < 166.4 kJ mol^{-1} for group 2 adducts; they are stronger for the ammonia adducts of group 2 cations by as much as a factor of 2. For both groups,
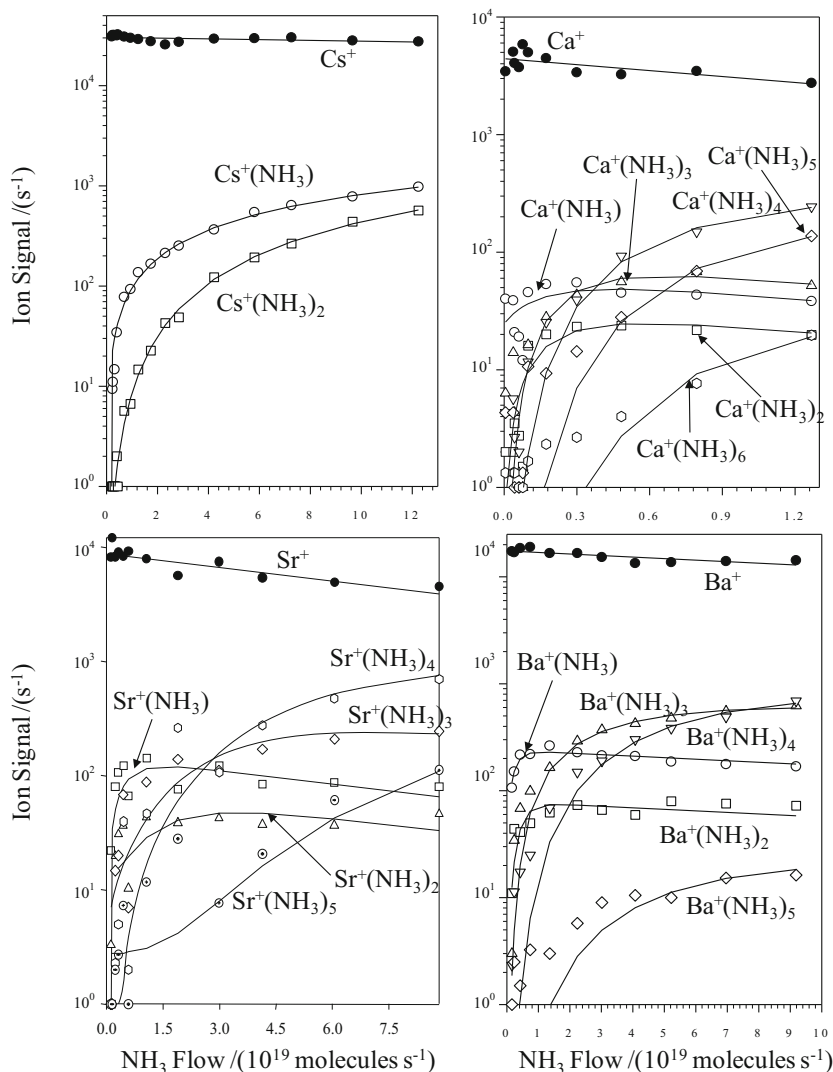
Figure 2. Ion profiles monitored for the sequential ligation of the bare alkali and alkali earth metal cations with ammonia in He buffer gas at 0.35 ± 0.01 Torr. Symbols represent experimental data and lines represent kinetic fits to that data

they decrease down the periodic table. The binding energy decrease less for group 1 than group 2 adducts: by almost 30% compared to 21% (ΔE_0 and ΔH_{298}, respectively) and by 39% compared to 15% (ΔG_{298}).

Of the ammonia adduct ions in Table 2, only $K^+(NH_3)$ appears to have received attention both experimentally and

theoretically. Our computed values of 90.4 and 62.1 kJ mol^{-1} for the bond dissociation enthalpy and Gibbs free energy of $K^+(NH_3)$ at 298 K, respectively, were compare with the values of 74.5 and 49.4 kJ mol^{-1} obtained in the first measurement in 1976 [22] from the temperature dependence of the equilibrium observed with a mass spectrometer equipped with a special

Table 1. Effective Bimolecular Rate Coefficients (In Units of cm^3 Molecule^{-1} s^{-1}) and Ligation Efficiencies for the Addition of One Ammonia Molecule to Alkali and Alkaline Earth Atomic Cations Measured at Room Temperature Using the ICP/SIFT Technique. Observed Higher-Order Adducts Formed by Sequential Ligation are Also Indicated. The Helium Buffer Gas Pressure was 0.35 ± 0.01 Torr. Uncertainties in the Rate Coefficients are Estimated to $\pm 30\%$. Included an Earlier Measurement in our Laboratory of the Ligation of mg$^+$ Using the SIFT Technique [7]

Reaction	Rate coefficient, k	Collision rate coefficient k_c	Ligation efficiency, k/k_c	Observed products
$Mg^+ + NH_3$	4.1×10^{-12}	2.5×10^{-9}	1.6×10^{-3}	$Mg^+(NH_3)_{1-5}$
$K^+ + NH_3$	1.2×10^{-12}	2.3×10^{-9}	5.2×10^{-4}	$K^+(NH_3)_{1-3}$
$Ca^+ + NH_3$	2.4×10^{-12}	2.3×10^{-9}	1.0×10^{-3}	$Ca^+(NH_3)_{1-6}$
$Rb^+ + NH_3$	5.5×10^{-13}	2.1×10^{-9}	2.6×10^{-4}	$Rb^+(NH_3)_{1-3}$
$Sr^+ + NH_3$	4.9×10^{-13}	2.1×10^{-9}	2.3×10^{-4}	$Sr^+(NH_3)_{1-5}$
$Cs^+ + NH_3$	1.0×10^{-13}	2.0×10^{-9}	5.0×10^{-5}	$Cs^+(NH_3)_{1-2}$
$Ba^+ + NH_3$	2.0×10^{-13}	2.0×10^{-9}	1.0×10^{-4}	$Ba^+(NH_3)_{1-5}$

Table 2. Summary of the Results of the DFT Calculations for the Formation of Adducts of Group 1 and Group 2 Cations with Ammonia, M^+NH_3 (C_{3v}). The Bond Length Refers to the Calculated Equilibrium M^+–N Bond Length. Also Included are the Computed Bond Energies with Zero-Point Correction, ΔE_0, as Well as Room Temperature Bond Enthalpies and Gibbs Free Energies, ΔH_{298} and ΔG_{298}. All Energies are in kJ Mol^{-1}

Adduct	Bond length (pm)	$-\Delta E_0$	$-\Delta H_{298}$	$-\Delta G_{298}$
$K^+(NH_3)$	278.9	86.1	90.4	62.1
$Rb^+(NH_3)$	297.1	73.9	77.8	53.0
$Cs^+(NH_3)$	318.5	61.3	65.0	38.4
$Ca^+(NH_3)$	241.0	161.4	166.5	136.0
$Sr^+(NH_3)$	260.2	133.0	137.7	110.7
$Ba^+(NH_3)$	275.8	127.2	131.7	105.3
$Ca^{2+}(NH_3)$	235.5	281.5	287.1	254.0
$Sr^{2+}(NH_3)$	254.0	231.9	237.2	204.6
$Ba^{2+}(NH_3)$	272.2	205.1	210.1	178.3

high pressure ion source and a potassium ion thermionic emitter. Other measurements and calculations range from 70 to 81 ± 9 kJ mol^{-1} at 0 K [23] including a CID measurement that found a value of 79 ± 7 kJ mol^{-1}.

The bond between the atomic cation and ammonia in both group 1 and 2 adducts is entirely or almost entirely electrostatic with no covalent character, and this is reflected in the low binding energies.

Electron localization and atomic charge data from the DFT calculations indicated that there is a minimal covalent binding between ammonia and the alkali and alkaline earth metal cations (see Supplementary Material). Electron delocalization from the metal cation to nitrogen is increased very slightly going from alkali (0–0.02e delocalization) to alkaline earth (0.04–0.08e delocalization) metal cations. This indicates that electrostatic binding is still the dominant mode of binding in the adduct. On the other hand, the covalent N–H bonds in ammonia show a high degree of electron delocalization, with 0.6–0.7e delocalized from hydrogen and 0.9–1.0e delocalized from nitrogen. Mulliken atomic charge data show a similar trend: the atomic charge of the metal cation is reduced from 0.95e in alkaline cations to 0.87e in alkaline earth cations. The charge on the nitrogen atom remains constant at -0.94e to -0.97e for all adducts.

A comparison of the reactivities of group 1 with group 2 cations provides an unique opportunity to evaluate the effect of a lone valence electron outside a noble gas electronic configuration with fully occupied orbitals on electron–electron repulsion with the free electron pair on ammonia.

Mono-adducts of singly charged group 1 and doubly charged group 2 cations offer a basis for this comparison when we view the nucleus and the electron shell as a tightly bound core that interacts with the ammonia ligand by electrostatic attraction. The bond length is indicative of how tightly the electron shell is bound to the nucleus. As expected, the adducts of doubly charged group 2 cations have 15% shorter bond lengths compared to singly charged group 1 cation adducts as increased charge binds the electron shell more tightly (see Table 2). The increased charge state yields shorter bonds and a three-fold increase in binding enthalpy (ΔH_{298}) for the doubly charged group 2 cation adducts.

Mono-adducts of singly charged group 2 cations present a curious compromise. The bond lengths for these complexes are very similar to those of doubly charged group 2 cations (which are less than 3% shorter; see Table 2), while the binding energies of the doubly charged adducts are increased by about a factor of 1.5. So, it appears that, while singly charged group 2 cations are able to achieve tighter binding than group 1 cations due to a higher core charge, substantial electron–electron repulsion between the valence electron and the ligand reduces the purely electrostatic binding energy of the adduct. Possibly, the metal center is polarized in mono-ligated group 2 adduct $M^+(NH_3)$ with its polarized s electron pointed opposite to the M–L bond, resulting in an electrostatic interaction similar to $\{e^-\}M^{2+}\ldots NH_3$.

Given the general interest by the chemical community in correlations of bond length/bond strength, we present in Figure 3 such a correlation for the group 1 and 2 metal cation/ammonia adducts that were calculated. Although there clearly is a trend of decreasing bond energy with increasing bond length within each group, we note that, in a very recent appraisal and critique of bond-length/bond-strength correlations, Kaupp et al. [24] have emphasized that such correlations, although often useful for obtaining equilibrium bond lengths, are strictly empirical and have no fundamental basis: "there is no law that requires that a deeper well with a higher D_e value should coincide with minima at shorter equilibrium distances."
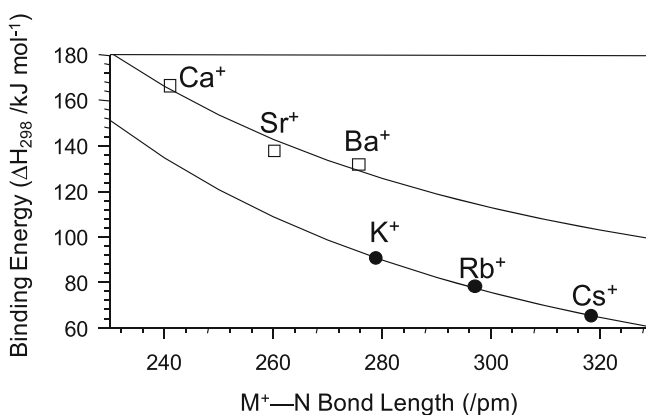
Figure 3. Correlation between calculated binding energies, ΔH_{298}, and M^+–N bond length (r). The lines correspond to a fit to $1/r^3$ ($a + b/r^3$) ([24] and see text)
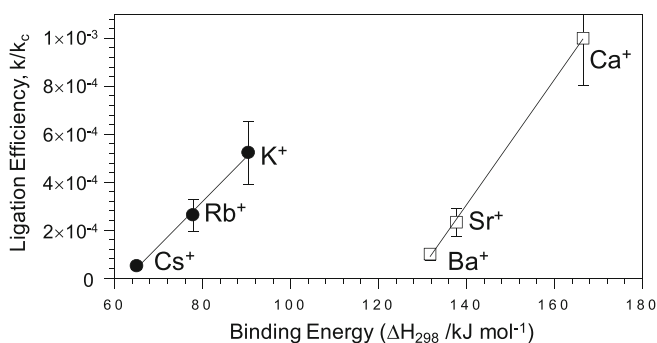
Figure 4. Correlation between measured ligation efficiency, k/k_c, and calculated binding energy. A linear fit has been applied. The fits are nearly parallel with binding energy ratios of $Ca^+/K^+ = 1.8$, $Sr^+/Rb^+ = 1.8$, and $Ba^+/Cs^+ = 2.0$

Correlation of Measured Rate Coefficients with Computed Binding Energies

The trend down the periodic table in the measured rate coefficient (see Table 1) is presented in Figure 4 in a correlation of the ligation efficiency, k/k_c, with the bond energy, ΔH_{298}, of the ammonia adduct (see Table 2).

Since the effective bimolecular rate coefficient of ligation $k(2) = k(3)n_{He}$, the steady-state model for ligation (see Introduction) predicts an efficiency of ligation, $k(2)/k_c$, given by Eq. (1),

$$k(2)/k_c = k_s\tau = k_s\tau_0 \, ((D + rRT)/rRT)^{s-1} n_{He} \qquad (1)$$

and when $D >> rRT$, the efficiency becomes directly dependent on D^{s-1}. For $s = 2$ coupled harmonic oscillators, this dependence becomes linear as shown in Figure 4 in which ΔH_{298} is taken as a measure of D, although a fit with $s = 3$ also accounts for the trend within experimental uncertainty. So, the correlation between the efficiency of ligation and the binding energy of the adduct ion can be said to be a consequence of the lifetime of the intermediate encounter complex against back dissociation, which is dependent on its well depth, D.

Higher-Order Ammonia Ligation and Electron Solvation

Table 1 includes a listing of the higher-order adducts that were observed to be formed by sequential ligation in the range of ammonia that was added to the flow tube. Remarkably, the alkaline earth cations were all seen to form larger solvation clusters with ammonia, $M^+(NH_3)_n$, with n up to 5 or 6, than those for alkali cations, with n up to 2 or 3. Why should that be so? One possibility is the occurrence of electron solvation in the higher adducts with ammonia of the solvated alkaline earth cations $Mg^+(NH_3)_n$, $Ca^+(NH_3)_n$, $Sr^+(NH_3)_n$, and $Ba^+(NH_3)_n$ with their s electron but not in $K^+(NH_3)_n$, $Rb^+(NH_3)_n$, and $Cs^+(NH_3)_n$ in which the metal cations have a rare-gas configuration.

Electron solvation has been characterized for hydrated alkaline earth cations, especially hydrated Mg^+ cations for which the formation of a magnesium dication and a hydrated electron $\{e^-\}Mg^{2+}$–$(H_2O)_n$ has been proposed by several authors [25–31]. We propose here that ammonia is also likely to support a solvated electron, viz. solvate the s electron present in the alkaline earth cations.

Can the onset of the contribution of the binding of the s electron to ammonia be discerned from the kinetics of higher-order ammonia ligation? Apparently so, from an inspection of the ligation rate profiles in Figure 2 which provides, for example, a comparison of the ligation of Cs^+ with that of Ba^+. Mono-solvation with ammonia is slow for both the cations but $k(Ba^+)/k(Cs^+) = 2$ in accordance with the ratio of computed binding enthalpies as expected from Eq. (1) with $s = 2$ or 3, within experimental uncertainty. The increase in the rate of addition of the second ammonia molecule is seen in Figure 2 to be much larger for $Ba^+(NH_3)$ than for $Cs^+(NH_3)$, or $\{e^-\}Ba^{2+}$–(NH_3), if we attribute the increased contribution to the binding energy of the second ammonia to s electron solvation. A kinetic fit of the data provided $k(Ba^+(NH_3))/(Cs^+(NH_3)) = 9.3$ with $k(Ba^+(NH_3)) = 2.6 \times 10^{-11}$ cm^3 molecule^{-1} s^{-1} and $k(Cs^+(NH_3)) = 2.8 \times 10^{-12}$ cm^3 molecule^{-1} s^{-1}. And again, for the third ammonia addition, $k(Ba^+(NH_3)_2)/(Cs^+(NH_3)_2) = 270$ with $k(Ba^+(NH_3)_2) = 2.7 \times 10^{-11}$ cm^3 molecule^{-1} s^{-1} and $k(Cs^+(NH_3)_2) = 1.0 \times 10^{-13}$ cm^3 molecule^{-1} s^{-1}. So, the measured kinetics, in addition to the observed formation of larger solvated clusters, is consistent with the occurrence of ammonia solvation of the s electron in the sequential binding of alkaline earth cations to ammonia.

Conclusions

We have extended our experimental approach for the assessment of the nature of the binding of ligands to atomic metal cations from measurements of the kinetics of adduct formation at room temperature to alkali (Rg) and alkali earth (Rg s^1) atomic cations adding to ammonia. A systematic decrease in the rate of addition of NH_3 was observed for both group 1 and 2 cations going down the periodic table. The computational studies also predict a decrease in the binding energy of the adduct ion and an increase in the bond separation going down groups 1 and 2 of the periodic table and provide some insight into the role of the extra s electron in the group 2 radical cations in ligand bonding. The correlation that is seen between the efficiency of ligation and the binding energy of the adduct ion can be attributed to the lifetime of the intermediate ligated encounter complex against back dissociation which is dependent on its well depth. Also, we have proposed the occurrence of ammonia solvation with the s electron in the alkaline earth cations. The observed formation of larger solvated adducts with the alkaline earth cations along with the measured kinetics is consistent with this proposition.

Acknowledgements

References

1. Blagojevic, V., Koyanagi, G.K., Bohme, D.K.: Ligation kinetics as a probe for relativistic effects in ion chemistry: gas-phase ligation of Ni^+, Pd^+ and Pt^+ at room temperature. Int J Mass Spectrom. **418**, 193–197 (2017)

2. Blagojevic, V., Koyanagi, G.K., Bohme, D.K.: Ligation kinetics as a probe for relativistic effects: ligation of atomic coinage metal cations with ammonia. Int J Mass Spectrom. **413**, 81–84 (2017)

3. Blagojevic, V., Lavrov, V.V., Bohme, D.K.: Ligation kinetics as a probe for relativistic effects in ion chemistry: gas-phase ligation of late atomic transition metal cations with OCS and CH_3Cl at room temperature. Int J Mass Spectrom. **429**, 101–106 (2018)

4. Blagojevic, V., Lavrov, V.V., Koyanagi, G.K., Bohme, D.K.: Ligation kinetics as a probe for gas-phase ligand field effects: Ligation of atomic transition metal cations with ammonia at room temperature. Eur J Mass Spectrom. 44–49 (25, 2019)

5. Blagojevic, V., Lavrov, V.V., Koyanagi, G.K., Bohme, D.K.: Early atomic transition metal cations reacting with ammonia at room temperature: H_2 elimination and NH_3 ligation kinetics across and down the periodic table. Int J Mass Spectrom. **435**, 181–186 (2019)

6. Koyanagi, G.K., Cheng, P., Bohme, D.K.: Gas-phase reactions of atomic lanthanide cations with ammonia: room-temperature kinetics and periodicity in reactivity. J Phys Chem A. **114**, 241–246 (2010)

7. Milburn, R.K., Baranov, V.I., Hopkinson, A.C., Bohme, D.K.: Sequential ligation of mg^+, Fe^+, $(c-C_5H_5)mg^+$ and $(c-C_5H_5)Fe^+$ with ammonia in the gas phase: transition from coordination to solvation in the sequential ligation of mg^+. J Phys Chem A. **102**, 9803–9810 (1998)

8. Rothe, E.W., Bernstein, R.B.: Total collision cross sections for the interaction of atomic beams of alkali metals with gases. J Chem Phys. **31**, 1619–1627 (1959)

9. "Ionization energies of atoms and atomic ions," in CRC Handbook of Chemistry and Physics, 98th Edition (Internet Version 2018), John R. Rumble, ed., CRC Press/Taylor & Francis, Boca Raton, FL

10. Shayesteh, A., Lavrov, V.V., Koyanagi, G.K., Bohme, D.K.: Reactions of atomic cations with methane: gas phase room-temperature kinetics and periodicities in reactivity. J Phys Chem A. **113**, 5602–5611 (2009)

11. Koyanagi, G.K., Bohme, D.K.: Gas-phase reactions of carbon dioxide with atomic transition-metal and main-group cations: room-temperature kinetics and periodicities in reactivity. J Phys Chem A. **110**, 1232–1241 (2006)

12. Good, A.: Classical semi-empirical rate equation for third order ion-molecule association reactions. Trans Faraday Soc. **67**, 3495–3502 (1971)

13. Koyanagi, G.K., Lavrov, V.V., Baranov, V.I., Bandura, D., Tanner, S.D., McLaren, J.W., Bohme, D.K.: A novel inductively coupled plasma/selected-ion flow tube mass spectrometer for the study of reactions of atomic and atomic oxide ions. Int J Mass Spectrom. **194**, L1–L4 (2000)

14. Koyanagi, G.K., Baranov, V.I., Tanner, S.D., Bohme, D.K.: An inductively-coupled plasma/selected-ion flow tube mass spectrometer study of the chemical resolution of isobaric interferences. J Anal At Spectrom. **15**, 1207–1210 (2000)

15. Mackay, G.I., Vlachos, G.D., Bohme, D.K., Schiff, H.I.: Studies of reactions involving $C_2H_x^+$ ions with HCN using a modified selected ion flow tube. Int J Mass Spectrom Ion Phys. **36**, 259–270 (1980)

16. Frisch, M.J., Trucks, G.W., Schlegel, H.B., Scuseria, G.E., Robb, M.A., Cheeseman, J.R., Montgomery Jr., J.A., Vreven, T., Kudin, K.N., Burant, J.C., Millam, J.M., Iyengar, S.S., Tomasi, J., Barone, V., Mennucci, B., Cossi, M., Scalmani, G., Rega, N., Petersson, G.A., Nakatsuji, H., Hada, M., Ehara, M., Toyota, K., Fukuda, R., Hasegawa, J., Ishida, M., Nakajima, T., Honda, Y., Kitao, O., Nakai, H., Klene, M., Li, X., Knox, J.E., Hratchian, H.P., Cross, J.B., Bakken, V., Adamo, C., Jaramillo, J., Gomperts, R., Stratmann, R.E., Yazyev, O., Austin, A.J., Cammi, R., Pomelli, C., Ochterski, J.W., Ayala, P.Y., Morokuma, K., Voth, G.A., Salvador, P., Dannenberg, J.J., Zakrzewski, V.G., Dapprich, S., Daniels, A.D., Strain, M.C., Farkas, O., Malick, D.K., Rabuck, A.D., Raghavachari, K., Foresman, J.B., Ortiz, J.V., Cui, Q., Baboul, A.G., Clifford, S., Cioslowski, J., Stefanov, B.B., Liu, G., Liashenko, A., Piskorz, P., Komaromi, I., Martin, R.I., Fox, D.J., Keith, T., Al-Laham, M.A., Peng, C.Y., Nanayakkara, A., Challacombe, M., Gill, P.M.W., Johnson, B., Chen, W., Wong, M.W., Gonzalez, C., Pople, J.A.: Gaussian 03, Revision D.01. Gaussian, Inc., Wallingford CT (2004)

17. Becke, A.D.: Density-functional exchange-energy approximation with correct asymptotic behavior. Phys Rev A. **38**, 3098–3100 (1988)

18. Lee, C., Yang, W., Parr, R.G.: Development of the Colle-Salvetti correlation-energy formula into a functional of the electron density. Phys Rev B. **37**, 785–789 (1988)

19. Andrae, D., Haeussermann, U., Dolg, M., Stoll, H., Preuss, H.: Energy-adjusted ab initio pseudopotentials for the 2nd and 3rd row transition-elements. Theor Chem Accounts. **77**, 123–141 (1990)

20. Dunning Jr., T.H., Hay, P.J.: In: Schaefer III, H.F. (ed.) Modern theoretical chemistry, vol. Vol. 3, pp. 1–28. Plenum, New York (1977)

21. Su, T., Chesnavich, W.J.: Parametrization of the ion–polar molecule collision rate constant by trajectory calculations. J Chem Phys. **76**, 5183–5185 (1982)

22. Davidson, W.R., Kebarle, P.: Binding energies and stabilities of potassium ion complexes from studies of the gas phase ion equilibria $K^+ + M = K^+M$. J Amer Chem Soc. **98**, 6133–6138 (1976)

23. Iceman, C., Armentrout, P.B.: Collision-induced dissociation and theoretical studies of K^+ complexes with ammonia: a test of theory for potassium ions. Int J Mass Spectrom. **222**, 329–349 (2003)

24. Kaupp, M., Danovich, D., Shaik, S.: Chemistry is about energy and its changes: a critique of bond-length/bond-strength correlations. Coord Chem Rev. **344**, 355–362 (2017)

25. Watanabe, H., Iwata, S., Hashimoto, K., Misaizu, F., Fuke, K.: Molecular-orbital studies of the structures and reactions of singly charged magnesium-ion with water clusters, $mg^+(H_2O)_n$. J Am Chem Soc. **117**, 755–763 (1995)

26. Berg, C., Beyer, M., Achatz, U., Joos, S., Niedner-Schatteburg, G., Bondybey, V.E.: Stability and reactivity of hydrated magnesium cations. Chem Phys. **239**, 379–392 (1998)

27. Reinhard, B.M., Niedner-Schatteburg, G.: Co-existence of hydrated electron and metal Di-Cation in $[Mg(H_2O)_n]^+$. Phys Chem Chem Phys. **4**, 1471–1477 (2002)

28. Siu, C.K., Liu, Z.F.: Ab initio studies on the mechanism of the size-dependent hydrogen-loss reaction in $mg^+(H_2O)_n$. Chem Eur J. **8**, 3177–3186 (2002)

29. Van der Linde, C., Akhgarnusch, A., Siu, C.K., Beyer, M.K.: Hydrated magnesium cations $mg^+(H_2O)_n$, n ≈ 20_60, exhibit chemistry of the hydrated electron in reactions with O_2 and CO_2. J Phys Chem A. **114**, 10174–10180 (2011)

30. Ončák, M., Taxer, T., Barwa, E., van der Linde, C., Beyer, M.K.: Photochemistry and spectroscopy of small hydrated magnesium clusters $Mg^+(H_2O)_n$, n = 1–5. J Chem Phys. **149**, 044309 (2018)

31. Taxer, T., Oncak, M., Barwa, E., van der Linde, C., Beyer, M.K.: Electronic spectroscopy and nanocalorimetry of hydrated magnesium ions $[Mg(H_2O)_n]^+$, n = 20–70. Spontaneous formation of a hydrated electron? Faraday Discuss. (2018). https://doi.org/10.1039/C8FD00204E